Scour Downstream of Grade-Control Structures

By Noel E. Bormann[1] and Pierre Y. Julien,[2] Members, ASCE

Abstract: A theoretical investigation of local scour downstream of grade-control structures based on two-dimensional jet diffusion and particle stability is experimentally verified. Turbulent jet diffusion reduces fluid velocity near the bed particles and equilibrium scour is obtained when noncohesive bed particles cannot be removed from the scour hole. Equilibrium scour depth is written as a function of velocity, flow depth and particle size. The theoretically derived equation is remarkably similar to the regression equations reported in the literature. The experimental investigation uses a large-scale physical model with unit discharge up to 2.5 m^2/s (27 sq ft/sec) and scour depths exceeding 1.4 m (4.6 ft). When combined with previous data sets at smaller scales, a total of 231 scour-depth measurements cover a wide variety of conditions: wall to vertical jets, small to large flow submergence, and various face angle slopes. The agreement between calculated scour depths and laboratory measurements is satisfactory considering the wide variety of configurations analyzed.

Introduction

Grade-control structures prevent excessive channel-bed degradation in alluvial channels. The erosive action of flowing water, however, causes significant downstream local scour, which may undermine these structures. Structural design considerations must therefore include adequate protective measures against local scour downstream of grade-control structures. In turn, appropriate protective measures can only be designed with a full understanding the mechanics, location and extent of downstream scour.

More than 50 years of laboratory measurements of scour depths under various flow conditions and structure configurations are available. Significant studies of local scour under a two-dimensional free jet downstream of hydraulic structures include those of Schoklitsch (1932), Veronese (1937), Jaeger (1939), Eggenberger (1943), Mueller and Eggenberger (1944), Hartung (1959), Damle et al. (1966), Smith and Strang (1967), Chee and Padiyar (1969), Chee and Kung (1971), Chee et al. (1972), Martins (1975), Laursen and Flick (1983), and Akashi and Saitou (1986). Experiments with two-dimensional submerged jets have been reported by Laursen (1952), Tarapore (1956), LeFeuvre (1965), Carstens (1966), Breusers (1967a, 1967b), Rajaratnam and Subramanya (1968), Altinbilek and Basmaci (1973), Altinbilek and Okyay (1973), and Rajaratnam (1981). Most existing scour-depth equations are summarized in Mason and Arumugam (1985). Maximum scour-depth equations were typically obtained from small-scale laboratory experiments with unit discharges less than 0.093 m^2/s (1 sq ft/sec) and scour depths not exceeding 0.8 m (2.9 ft).

The purpose of this paper is twofold: (1) Derive an equilibrium scour equation based on the concepts of jet diffusion and particle stability in scour

[1]Asst. Prof., Dept. of Civ. Engrg., Gonzaga Univ., Spokane, WA 99258.
[2]Assoc. Prof., Dept. of Civ. Engrg., Colorado State Univ., Fort Collins, CO 80523.

Note. Discussion open until October 1, 1991. To extend the closing date one month, a written request must be filed with the ASCE Manager of Journals. The manuscript for this paper was submitted for review and possible publication on February 28, 1990. This paper is part of the ***Journal of Hydraulic Engineering***, Vol. 117, No. 5, May, 1991. ©ASCE, ISSN 0733-9429/91/0005-0579/$1.00 + $.15 per page. Paper No. 25829.

holes downstream of grade-control structures; and (2) test the equation with large-scale experiments with local scour-depth measurements up to 1.4 m (4.5 ft).

Flow Characteristics Downstream of Grade-Control Structures

Consider the grade-control structure sketched in Fig. 1. As the flow downstream from A' enters the tailwater Y_t, it forms a neutrally buoyant jet with average velocity U_o and thickness Y_o, which diffuses between points A' and B'. Flow separates from the structure at point A' and a vortex is formed in the separation zone. With reduced pressure between points A' and C' the jet deviates toward the boundary at an angle β' because of the Coanda effect discussed by Newman (1961), Bourque and Newman (1960), and Rajaratnam and Subramanya (1968). The diffused flow velocity U_b in the vicinity of B' exerts a shear stress on bed sediment particles. When the applied shear stress exceeds the critical shear stress, sediment is removed from the impingement region and local scour progresses. Note that for live-bed scour, scour occurs when the rate of particle removal exceeds the transport rate into the scour hole.

Equilibrium conditions are asymptotically reached as the rate of scour approaches zero. For clear-water scour, the diffusion length L_s increases as scour progresses, and the diffused velocity U_b decreases until the hydrodynamic force exerted on the particles no longer removes them out of the scour hole. The maximum scour depth D_s can then be determined from the diffusion length L_s, the jet angle β' between A' and B', and the drop height D_p of the grade-control structure:

$$D_s = L_s \sin \beta' - D_p \quad (1)$$

Both prototype and laboratory model flow fields are not exactly two-dimensional because of sidewall effects. The three-dimensional character of the flow is, however, considered small compared to the dominant two-dimensional flow field generated from wide rectangular grade-control structures. The local scour resulting from various configurations of two-dimen-

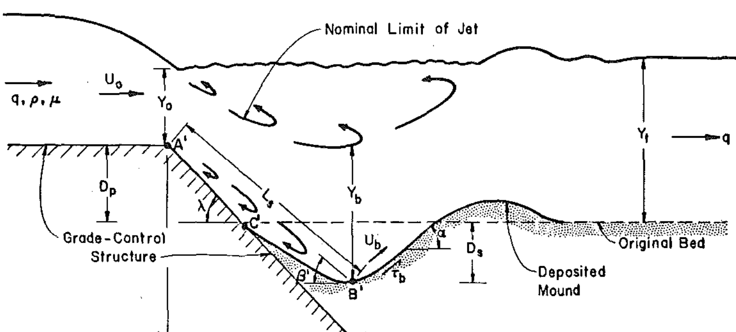

FIG. 1. Definition Sketch for Scour Downstream of Grade-Control Structures

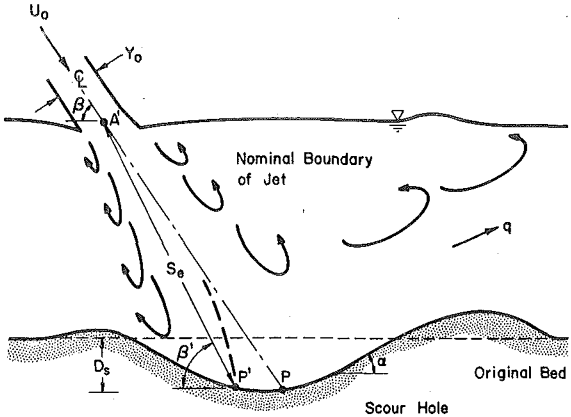

FIG. 2. Path of Free Jet

sional jets depends on: (1) The path of the jet; (2) the jet diffusion through tailwater; and (3) the stability of particles in the scour hole.

Jet Trajectory

Two types of jets must be considered separately, submerged jets and free jets. Under the partially submerged flow conditions in Fig. 1, the jet is deflected by both gravity and the Coanda effect. A dimensional analysis of the jet deflection angle β' for submerged jets yields the following dimensionless parameters:

$$\beta' = f\left(\frac{D_p + Y_o}{Y_o}, \frac{U_o^2}{gY_o}, \frac{Y_o}{Y_t}, \sin\lambda\right) \quad (2)$$

where g = the gravitational acceleration; and λ = the face angle of the grade-control structure. A specific relationship of the variables in Eq. 2 is empirically obtained from experimental data since the energy losses and pressure distributions surrounding the jet cannot directly be accounted for.

A free jet (Fig. 2) occurs when a jet of water is surrounded by atmospheric pressure as it enters the tailwater. Analysis of the free-jet data from Yuen (1984) shows that the angle β' can be approximated by the impinging jet angle β. From the investigations of Akashi and Saitou (1986), Rajaratnam (1981), Tarapore (1956), and Yuen (1984), an analysis of the scour-hole geometry suggests that the downstream face slope angle α is also approximately equal to the jet angle β', and thus $\alpha \approx \beta'$ serves as a first approximation for the downstream face slope of the scour hole.

Jet Diffusion

The characteristics of two-dimensional jets passing through tailwater and impinging on a smooth rigid boundary have been investigated by Beltaos and Rajaratnam (1973) with results quite similar to those of Albertson et al. (1950). The established flow region of the jet is defined as:

$$L_s \geq C_d^2 Y_o \quad (3)$$

where the jet diffusion coefficient C_d depends on inlet conditions and remains nearly independent of the jet orientation. Values of C_d suggested by Albertson et al. (1950), Beltaos and Rajaratnam (1973), and Yuen (1984) range from 2.0 to 2.4 for well-formed jets and depend on inlet conditions.

The diffused jet velocity in the scour hole U_b and the diffused jet thickness Y_b after the jet impinges on a boundary can be closely approximated by:

$$U_b = C_d U_o \left(\frac{Y_o}{L_s}\right)^{0.5} \quad \ldots\ldots (4)$$

and

$$Y_b = \frac{U_o}{U_b} Y_o \quad \ldots\ldots (5)$$

The location of the velocity U_b depends on the boundary roughness (Kobus et al., 1979) described by particle size, which also appears to influence the shape of the scour hole. The maximum downstream face slope angle α of the scour hole occurs near the point of maximum shear stress predicted by Beltaos and Rajaratnam (1973).

Particle Stability

The stability analysis of a noncohesive particle in a scour hole defines equilibrium conditions between the particle weight and the hydrodynamic force generated by the diffused jet velocity. The bed shear stress τ_b can be written as a function of the diffused jet velocity U_b as:

$$\tau_b = C_f \rho U_b^2 \quad \ldots\ldots (6)$$

where C_f = the local friction coefficient; and ρ = the mass density of water. Several investigations reported in Bogardi (1974) indicate that C_f can be expressed as a simple function of relative roughness:

$$C_f = \frac{\theta_{cr}}{B} \left(\frac{d_s}{Y_b}\right)^x \quad \ldots\ldots (7)$$

where d_s = the sediment size and the values of B and x are given in Table 1. The critical value of the Shields number θ_{cr} for noncohesive particles can be obtained from the Shields diagram for hydraulically smooth and rough flow conditions. For fully developed turbulent flows over a rough boundary, θ_{cr} is approximately constant at 0.047. In a developing boundary layer θ_{cr} is reported as 0.11. The value θ_{cr} relates to the critical shear stress τ_{cr} corre-

TABLE 1. Parameters of Local Friction Coefficient

Source (1)	Coefficient B (2)	Exponent x (3)
Straub (1953)	2.2	0.33
Bogardi (1974a)	0.001[a]	1.20
Bogardi (1974b)	2.9	0.19
Neill (1968)	2.0	0.33

[a]In the original equation, an additional term also influences B.

sponding to the beginning of particle motion on a horizontal bed by:

$$\tau_{cr} = \theta_{cr}(\gamma_s - \gamma)d_s \quad \ldots\ldots (8)$$

where γ_s = the specific weight of sediment; and γ = the specific weight of water.

A complete three-dimensional analysis of the forces and moments exerted on a single particle has been presented by Stevens and Simons (1971). The critical shear stress τ_b required for sediment particles to move upslope at an angle α in the downstream direction is obtained when the stability factor is unity for an embankment angle of $-\alpha$ and a flow angle of 90°. The corresponding ratio of shear stresses for a sloping bed τ_b versus a flat bed τ_{cr} is:

$$\frac{\tau_b}{\tau_{cr}} = \frac{\sin(\phi + \alpha)}{\sin\phi} \quad \ldots\ldots (9)$$

where ϕ = the submerged angle of repose of the granular material.

Under equilibrium scour conditions, the diffused distance to maximum scour depth L_s is obtained after combining Eqs. 4, 5, 6, 7, 8, and 9, and solving for L_s:

$$L_s = \left[\frac{\rho \sin\phi}{B(\gamma_s - \gamma)\sin(\phi + \alpha)}\right]^{2/(2+x)} C_d^2 \frac{Y_o^{(2-x)/(2+x)} U_o^{4/(2+x)}}{d_s^{(2-2x)/(2+x)}} \quad \ldots\ldots (10)$$

The numerical value of each exponent in Eq. 10 depends solely on x. Experimental work by Kobus et al. (1979) indicated that the shear stress at a rough boundary is dependent on the relative roughness of the impinging jet raised to the exponent 0.41; apparently, x also depends on flow geometry and bed porosity. For the situation addressed here, predictive results are improved when $x = 0.5$, which falls within the range of x values listed in Table 1.

The corresponding equilibrium scour depth D_s is then calculated directly from Eqs. 10 and 1:

$$D_s = \left\{\left[\frac{\gamma \sin\phi}{\sin(\phi + \alpha)B(\gamma_s - \gamma)g}\right]^{0.8} \frac{C_d^2 Y_o^{0.6} U_o^{1.6}}{d_s^{0.4}} \sin\beta'\right\} - D_p \quad \ldots\ldots (11)$$

Eq. 11 can be rewritten as:

$$D_s + D_p = Kq^{0.6} \frac{U_o}{g^{0.8} d_s^{0.4}} \sin\beta' \quad \ldots\ldots (12)$$

where $q = U_o Y_o$; and $K = C_d^2 [\gamma \sin\phi / \sin(\phi + \alpha) B(\gamma_s - \gamma)]^{0.8}$.

This equilibrium scour depth (Eq. 12) is compared in Table 2 with empirical local scour equations in the power form proposed by Mason and Arumugam (1985):

$$D_s + D_p = K \frac{q^a U_o^b \Delta H^c Y_i^d \beta'^e}{g^f d_s^i} \quad \ldots\ldots (13)$$

where a, b, c, d, e, f, and i = exponents of the scour equation; ΔH = the head drop across the structure (m); g = the gravitational acceleration (m/s^2); d_s = the effective sediment size (m); and the other variables defined

TABLE 2. Summary of Local Scour Equations: $D_s + D_p = Kq^a U_o^b \Delta H^c Y^d \beta'^e / g^f d_s^i$

Investigator (1)	K (2)	a (3)	b (4)	c (5)	d (6)	e (7)	f (8)	i (9)
Schoklitsch (1932)	0.5	0.57	0	0.2	NA	NA	NA	0.32
Veronese (1937a)	0.2	0.54	0	0.225	NA	NA	NA	0.42
Veronese (1937b)	1.9	0.54	0	0.225	NA	NA	NA	NA
Jaeger (1939)	0.6	0.50	0	0.25	0.33	NA	NA	0.33
Eggenberger (1943)	1.4	0.60	0	0.50	NA	NA	NA	0.40
Mueller and Eggenberger (1944)	—[a]	0.60	0	0.50	NA	NA	0.8	0.40
Hartung (1959)	1.4	0.64	0	0.36	NA	NA	NA	0.32
Damle et al. (1966)	0.6	0.50	0	0.50	NA	NA	NA	NA
Chee and Padiyar (1969)	2.1	0.67	0	0.18	NA	NA	NA	0.06
Chee and Kung (1971)	1.7	0.60	0	0.20	NA	NA	NA	0.10
Chee et al. (1972)	1.9	0.60	0	0.20	NA	−0.4	NA	0.10
Martins (1975)	1.5	0.60	0	0.10	NA	NA	NA	NA
Chee and Yuen (1985)	0.6	0.45	0.55	NA	NA	1.0[b]	NA	0.10
Mason and Arumugam (1985)[c]	3.27	0.60	0	0.05	0.15	NA	0.30	0.10
Bormann (1988a)	0.7	0.45	1.0	NA	0.12	0.66[b]	0.73	0.30
Eq. 12	—[d]	0.60	1.0	NA	NA	1.0[b]	0.8	0.4

[a]K depends on jet configuration.
[b]Uses sin β'.
[c]Summary of many previous equations, values of exponent vary with H.
[d]Constant depends on inlet geometry and sediment properties.
Note: NA = not applicable.

earlier are in metric units. Most empirical scour-depth studies listed in Table 2 are concerned with vertically impinging jets, and only three studies (Chee and Kung 1971; Chee et al. 1972; and Yuen 1984) relate to nonvertical free-jet conditions. Jaeger (1939), Eggenberger (1943), and Mueller and Eggenberger (1944) studied horizontal jets entering tailwater. Other studies of submerged slightly inclined jets have established the similarity of scour-hole geometry and dependence on flow conditions (e.g., Farhoudi and Smith 1985; Rajaratnam 1981). The equation of Mason and Arumugam (1985), developed from an extensive literature review, appears to be representative of previous investigations using vertical free jets. The empirical equation of Chee and Yuen (1985), and a summary of Yuen (1984), attempts to incorporate jet diffusion into the prediction of local scour caused by two-dimensional jets. An empirical equation developed by Bormann (1988a) accounts for jet diffusion and is applicable to free and submerged jets at any orientation. Eq. 12 proposed here reflects both jet diffusion and the stability of sediment particles in a scour hole.

Examination of Table 2 leads to several conclusions: (1) The agreement of exponent a is remarkable; (2) the value of exponent i is quite similar to approximately half of the equations listed, the other half have values of 0.1; and (3) the proposed Eq. 12 is comparable to the other equations listed in Table 2.

LARGE-SCALE EXPERIMENTS

A large-scale experimental investigation with unit discharges ranging from 0.3 to 2.5 m^2/s (3 to 27 sq ft/sec) and maximum scour depths reaching 1.4

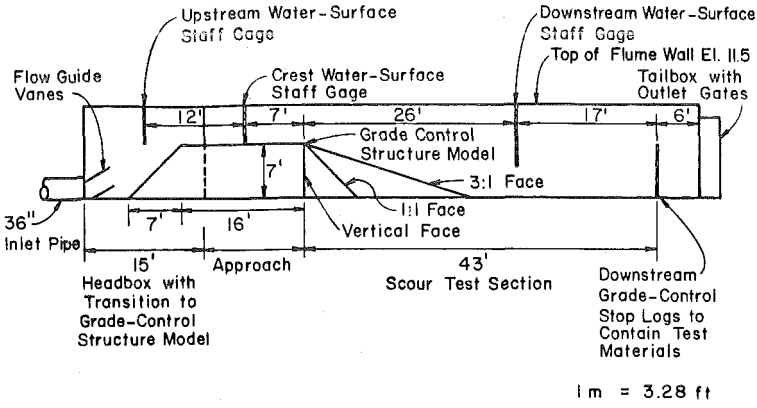

FIG. 3. Sketch of Large-Scale Test Flume

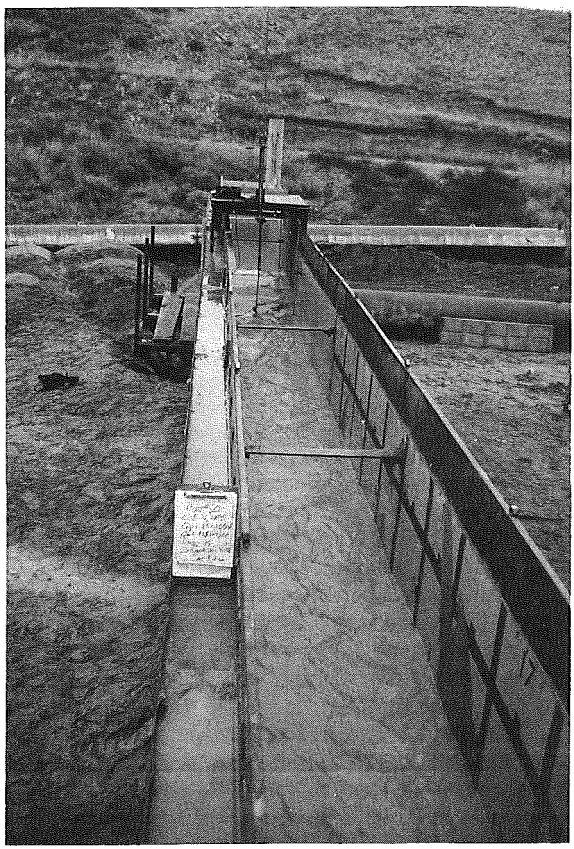

FIG. 4(*a*). Test Flume at Low Flow

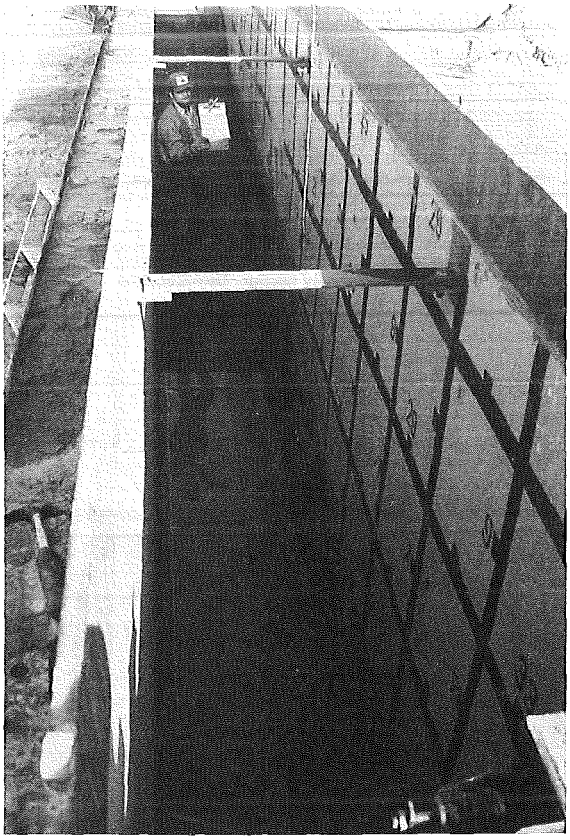

FIG. 4(*b*). Test Flume with Scour Depth Approaching 2 m

m (4.6 ft), was carried out using a large outdoor flume at the Colorado State University Engineering Research Center. The installation consisted of a headbox/inlet, an approach section, a scour-test section, and a tailbox/outlet (see Fig. 3). A 0.91-m (3-ft) diameter mixed flow pump supplied up to 2.7 m^3/s (75 cu ft/sec) to the flume test section. The flume had an overall depth of 3.5 m (11.5 ft), an overall length of 27.4 m (90 ft), and a width of 0.91 m (3 ft). The elevation of the grade-control structure model crest was set at 2.13 m (7 ft) above the flume floor. When scaled according to the Froude similitude criteria, the model scale is much larger than any previously reported tests. In fact, at this scale, the model tests overlap some prototype scour values, as discussed in Bormann (1988b).

The scour test section is defined from the crest of the grade-control structure model. A steel plate was welded to the flume walls to form the various structure face slopes tested. The scour test section exceeded 13 m (43 ft) from the crest to the downstream grade-control for the model. Downstream stop logs controlled the drop height from the crest to the sediment bed level. The water in the flume flowed over the stop logs into the tailbox, which

TABLE 3. Summary of Experimental Data

Test number (1)	Y_o (m) (2)	U_o (m/s) (3)	D_p (m) (4)	Y_t (m) (5)	D_s (m) (6)	X_s (m) (7)	d_{90} (mm) (8)	d_{50} (mm) (9)	λ radian (10)	Relative submergence (%) (11)	q (m^2/s) (12)	β' radian (13)	L_s (m) (14)
1	0.94	2.38	0.15	1.25	1.12	6.10	1.58	0.30	0.79	90	2.25	0.21	6.23
2	0.94	2.38	0.15	1.25	1.02	6.10	1.58	0.30	0.79	90	2.25	0.19	6.21
3	0.94	2.38	0.15	0.25	1.02	6.10	1.58	0.30	0.79	90	2.25	0.19	6.21
4	0.57	3.92	0.15	0.98	1.46	6.10	1.58	0.30	0.79	71	2.22	0.26	6.31
5	0.57	3.92	0.15	0.88	1.40	7.93	1.58	0.30	0.79	63	2.22	0.19	8.08
6	0.88	1.95	0.15	1.07	1.01	6.71	1.58	0.30	0.79	86	1.72	0.17	6.81
7	0.88	1.95	0.15	1.07	1.10	4.88	1.58	0.30	0.79	86	1.72	0.25	5.04
8	0.88	1.95	0.15	1.07	1.08	5.49	1.58	0.30	0.79	86	1.72	0.22	5.62
9	0.48	3.58	0.15	0.82	1.16	5.49	1.58	0.30	0.79	67	1.71	0.23	5.64
10	0.48	3.58	0.15	0.82	1.07	5.49	1.58	0.30	0.79	66	1.71	0.22	5.62
11	0.48	3.58	0.15	0.82	1.14	6.10	1.58	0.30	0.79	66	1.71	0.21	6.23
12	0.48	3.58	0.15	0.82	1.28	6.10	1.58	0.30	0.79	66	1.71	0.23	6.26
13	1.19	1.52	0.25	1.50	0.72	4.27	1.58	0.30	0.79	93	1.81	0.22	4.38
14	0.75	2.38	0.25	1.09	0.98	7.32	1.58	0.30	0.79	70	1.78	0.17	7.42
15	0.46	3.84	0.25	0.92	1.30	6.10	1.58	0.30	0.79	56	1.78	0.25	6.29
16	1.16	2.07	0.25	1.44	0.55	6.10	1.58	0.30	0.79	91	2.40	0.13	6.15
17	0.55	4.23	0.25	0.91	1.32	6.71	1.58	0.30	0.79	52	2.32	0.23	6.89
18	1.17	1.65	0.05	1.28	0.66	4.27	1.58	0.30	0.79	93	1.93	0.17	4.33
19	0.79	2.87	0.05	0.94	1.08	6.71	1.58	0.30	0.79	70	2.27	0.17	6.80
20	0.54	4.27	0.05	0.71	1.21	6.71	1.58	0.30	0.79	51	2.32	0.19	6.82
21	0.52	3.73	0.05	0.86	0.97	4.88	1.58	0.30	0.79	71	1.94	0.21	4.98
22	0.53	3.76	0.05	0.74	1.26	7.93	1.58	0.30	0.79	62	1.99	0.16	8.03
23	1.13	2.19	0.23	1.46	0.96	4.27	1.71	0.45	0.79	92	2.47	0.27	4.43
24	0.58	3.97	0.23	1.08	1.06	6.71	1.71	0.45	0.79	70	2.32	0.19	6.83
25	0.55	4.23	0.23	0.88	1.39	7.93	1.71	0.45	0.79	53	2.32	0.20	8.09
26	1.04	1.37	0.23	1.26	0.70	3.66	1.71	0.45	0.79	92	1.42	0.25	3.77
27	0.43	3.40	0.23	0.87	0.89	4.88	1.71	0.45	0.79	70	1.46	0.22	5.00
28	0.40	3.70	0.23	0.66	1.10	4.88	1.71	0.45	0.79	47	1.46	0.27	5.06
29	0.69	0.88	0.23	0.93	0.27	2.44	1.71	0.45	0.79	96	0.61	0.20	2.49
30	0.34	1.71	0.23	0.59	0.29	3.05	1.71	0.45	0.79	72	0.58	0.17	3.09
31	0.20	3.00	0.23	0.45	0.56	3.66	1.71	0.45	0.79	46	0.60	0.21	3.74
32	0.19	3.11	0.23	0.39	0.62	3.05	1.71	0.45	0.79	33	0.59	0.27	3.17
33	0.25	1.36	0.23	0.48	0.10	1.83	1.71	0.45	0.79	72	0.34	0.18	1.86
34	0.14	2.47	0.23	0.39	0.15	1.83	1.71	0.45	0.79	48	0.34	0.20	1.87
35	0.12	2.80	0.23	0.30	0.39	2.44	1.71	0.45	0.79	20	0.33	0.25	2.52
36	0.12	2.87	0.23	0.28	0.93	1.83	1.71	0.45	0.79	15	0.33	0.56	2.16
37	1.17	2.01	0.38	1.65	0.58	4.27	1.71	0.45	1.57	95	2.36	0.22	4.37
38	0.58	3.97	0.38	1.22	0.94	8.54	1.71	0.45	1.57	70	2.32	0.15	8.64
39	0.85	1.71	0.38	1.30	0.25	1.22	1.71	0.45	1.57	94	1.46	0.48	1.37
40	0.43	3.41	0.38	1.03	0.59	6.10	1.71	0.45	1.57	73	1.46	0.16	6.17
41	0.39	3.77	0.38	0.78	1.05	5.49	1.71	0.45	1.57	45	1.46	0.25	5.67
42	0.35	4.22	0.38	0.60	1.43	4.88	1.71	0.45	1.57	24	1.48	0.36	5.20
43	0.16	3.90	0.38	0.79	0.31	4.27	1.71	0.45	1.57	68	0.62	0.16	4.32
44	0.20	2.96	0.38	0.58	0.47	3.05	1.71	0.45	1.57	42	0.59	0.27	3.17
45	0.18	3.27	0.38	0.48	0.64	3.05	1.71	0.45	1.57	20	0.58	0.32	3.21
46	0.16	3.74	0.38	0.39	0.88	4.27	1.71	0.45	1.57	1	0.60	0.29	4.45
47	0.31	0.91	0.38	0.71	0.28	0.61	1.71	0.45	1.57	91	0.29	0.83	0.90
48	0.22	1.39	0.38	0.60	0.14	3.05	1.71	0.45	1.57	70	0.30	0.17	3.09
49	0.12	2.45	0.38	0.51	0.18	3.05	1.71	0.45	1.57	42	0.31	0.18	3.10
50	0.11	2.61	0.38	0.44	0.28	1.83	1.71	0.45	1.57	20	0.29	0.35	1.94
51	0.09	3.20	0.38	0.29	1.39	1.22	1.71	0.45	1.57	1	0.30	0.97	2.15
52	0.26	1.13	0.08	0.45	0.23	1.22	1.71	0.45	1.57	95	0.29	0.24	1.26

TABLE 3. (*Continued*)

(1)	(2)	(3)	(4)	(5)	(6)	(7)	(8)	(9)	(10)	(11)	(12)	(13)	(14)
53	0.14	2.09	0.08	0.29	0.36	1.83	1.71	0.45	1.57	70	0.29	0.23	1.88
54	0.12	2.45	0.08	0.24	0.46	2.44	1.71	0.45	1.57	50	0.30	0.22	2.50
55	0.46	1.34	0.08	0.78	0.11	0.61	1.71	0.45	1.57	94	0.62	0.29	0.64
56	0.17	3.71	0.08	0.47	0.40	2.44	1.71	0.45	1.57	70	0.63	0.19	2.48
57	0.22	2.68	0.08	0.37	0.53	3.05	1.71	0.45	1.57	56	0.59	0.20	3.11
58	1.01	1.46	0.08	1.18	0.29	1.83	1.71	0.45	1.57	94	1.47	0.20	1.86
59	0.38	3.86	0.08	0.69	0.77	4.27	1.71	0.45	1.57	70	1.45	0.20	4.35
60	0.25	1.36	0.23	0.48	0.12	1.83	1.71	0.45	1.57	71	0.34	0.19	1.86
61	0.14	2.50	0.23	0.38	0.21	1.83	1.71	0.45	1.57	44	0.34	0.24	1.88
62	0.12	2.80	0.23	0.29	0.42	1.83	1.71	0.45	1.57	19	0.32	0.34	1.94
63	0.62	0.94	0.23	0.87	0.17	1.83	1.71	0.45	1.57	95	0.59	0.22	1.87
64	0.35	1.66	0.23	0.58	0.40	3.66	1.71	0.45	1.57	70	0.58	0.17	3.71
65	0.20	2.92	0.23	0.45	0.52	3.66	1.71	0.45	1.57	45	0.59	0.20	3.73
66	0.19	3.11	0.23	0.39	0.62	2.44	1.71	0.45	1.57	33	0.59	0.33	2.58
67	1.10	1.34	0.23	1.34	0.37	3.05	1.71	0.45	1.57	93	1.47	0.19	3.11
68	0.34	4.45	0.23	0.89	0.70	4.88	1.71	0.45	1.57	74	1.53	0.19	4.96
69	0.40	3.59	0.23	0.67	1.04	4.27	1.71	0.45	1.57	49	1.44	0.29	4.45
70	1.08	1.34	0.00	1.15	0.28	1.83	1.71	0.45	1.57	94	1.45	0.15	1.85
71	0.31	4.65	0.00	0.65	0.70	3.05	1.71	0.45	1.57	70	1.45	0.23	3.13
72	0.67	0.88	0.00	0.70	0.16	0.61	1.71	0.45	1.57	94	0.59	0.25	0.63
73	0.21	2.84	0.00	0.33	0.52	3.05	1.71	0.45	1.57	61	0.60	0.17	3.09
74	1.18	2.01	0.00	1.19	0.60	3.05	1.71	0.45	1.57	89	2.37	0.19	3.11
75	0.54	3.79	0.00	0.79	0.89	4.27	1.71	0.45	1.57	62	2.04	0.21	4.36
76	1.18	1.89	0.08	1.30	0.47	3.05	1.71	0.45	1.57	91	2.23	0.18	3.10
77	0.56	3.89	0.08	0.90	1.16	6.10	1.71	0.45	1.57	70	2.18	0.20	6.22
78	1.16	1.98	0.23	1.41	0.59	3.66	1.71	0.45	1.57	91	2.31	0.22	3.75
79	0.61	4.05	0.23	1.05	0.94	6.10	1.71	0.45	1.57	68	2.45	0.19	6.21
80	1.13	2.16	0.23	1.47	0.59	4.27	1.71	0.45	0.32	91	2.44	0.19	4.35
81	1.10	1.34	0.23	1.35	0.30	1.83	1.71	0.45	0.32	94	1.47	0.28	1.90
82	0.42	3.36	0.23	0.85	0.71	4.27	1.71	0.45	0.32	70	1.42	0.22	4.37
83	0.62	0.94	0.23	0.99	0.15	1.22	1.71	0.45	0.32	96	0.59	0.30	1.28
84	0.24	2.53	0.23	0.58	0.57	2.44	1.71	0.45	0.32	71	0.61	0.32	2.56
85	0.19	2.91	0.23	0.44	1.52	5.49	1.71	0.45	0.32	44	0.55	0.31	5.76
86	0.16	2.08	0.23	0.46	0.48	2.44	1.71	0.45	0.32	69	0.33	0.28	2.54
87	0.13	2.41	0.23	0.37	0.56	2.44	1.71	0.45	0.32	44	0.32	0.31	2.56
88	0.11	2.65	0.23	0.28	0.97	3.66	1.71	0.45	0.32	18	0.29	0.32	3.85

controlled the tailwater depth in the test section. A point gage mounted on a mechanical carriage was used to measure the scoured bed elevations in the center of the flume. Water-surface elevations were measured using three staff gages. Fig. 4 shows two photographs of the experimental flume. In Fig. 4(*a*), a small test flow of 0.28 m^2/s (3.1 sq ft/sec) is shown. Fig. 4(*b*) shows the flume after a test flow of 2.32 m^2/s (25 sq ft/sec). The structure slope is set at 3H:1V and scour depth in this particular run exceeded 1.98 m (6.5 ft) and reached the flume's bottom panel.

Details on model operation, data collection procedures and accuracy are available in Bormann (1988a). The data set contains 99 tests, of which 11 were deleted because scour exposed the flume bottom, leaving 88 equilibrium scour-depth measurements summarized in Table 3. The parameters listed in Table 3 are sketched in Fig. 1, while d_{50} and d_{90} denote the standard sieve diameter for which 50% and 90% of the particles are finer. Flow submergence is calculated by dividing the tailwater depth above the structure crest

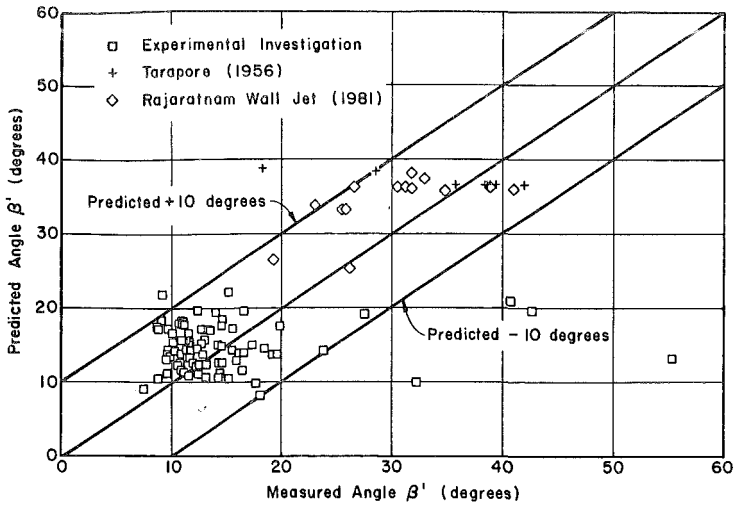

FIG. 5. Comparison of Measured and Calculated Jet Angle β′

by the flow depth on the structure. Note that the flow depth on the structure differs from the thickness of the jet entering tailwater because the pressure distribution is not hydrostatic.

The data set in Table 3 has been combined with other experimental data sets to determine the jet diffusion angle β′. Tarapore (1956) and Rajaratnam (1981) obtained a measurement of β′ for deeply submerged jets, while Table 3 covers tailwater depths not exceeding the inflow water depth. The data set including 109 data points covers a wide spectrum of submergence conditions, both for reattached wall jets with variable drop height and for wall jets with zero drop height. The angle β′ in radians is obtained by regression analysis:

$$\beta' = 0.316 \sin \lambda + 0.15 \ln \left(\frac{D_p + Y_o}{Y_o} \right) + 0.13 \ln \left(\frac{Y_t}{Y_o} \right) - 0.05 \ln \left(\frac{U_o}{\sqrt{g Y_o}} \right) \quad \ldots\ldots (14)$$

The values of the coefficients of this regression equation ($R^2 = 0.906$ and mean adjusted error = 0.074) indicate that β′ increases primarily with face slope angle, and varies slightly with drop height, tailwater depth and approach Froude number. Fig. 5 compares the results from Eq. 14 with the observed values of β′ for submerged reattached wall jets. The mean adjusted prediction error for β′ is less than 0.1 radian (approximately 5°), and only six data points lie beyond error bands of ±10°.

After combining the data set in Table 3 with previously published measurements of equilibrium scour depth, a total of 231 observations under a wide variety of flow conditions and structure configurations were available to test the applicability of Eqs. 10 and 11. The flow conditions include ver-

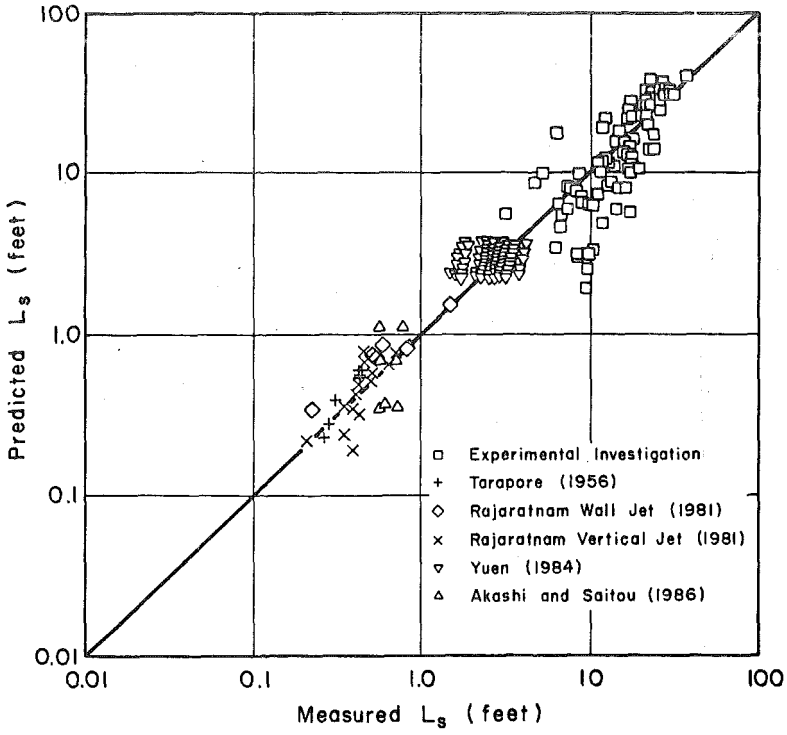

FIG. 6. Comparison of Measured and Calculated Diffusion Length L_s

tical jets, wall jets, free overfall jets, submerged jets and partially submerged flow over large scale drop structures with vertical and inclined (3H:1V and 1H:1V) face slopes. Fig. 6 compares observed diffusion lengths L_s with the theoretical values calculated from Eq. 10. The following numerical values of the parameters were selected based on the evaluation of relevant flow and particle conditions: $x = 0.5$, $\alpha = \beta'$, $\gamma_s = 2.7\gamma$, $B = 2.0$, $d_s = d_{90}$, $C_d = 1.8$, and $\phi = 25°$. Note that the parameter $x = 0.5$ determines the values of the exponents of Eq. 10 which were previously discussed in Table 2. The remaining parameters influence the diffusion length L_s and the scour depth D_s solely through the parameter K from Eq. 12. Identical values of K can be obtained with a different set of parameters. Fig. 7 compares the observed scour depths with the calculated scour depths from Eq. 11.

It is found from Figs. 6 and 7, that the diffusion length L_s can be determined more accurately than the scour depth D_s. This expected result stems from the fact that scour depth from Eq. 11 is relatively sensitive to the angle β' at low values of β'. Further research on the separation zone, the Coanda effect, and the natural instability and oscillations of plunging jets may theoretically provide better estimates of β'.

CONCLUSIONS

Local scour downstream of grade-control structures is examined theoret-

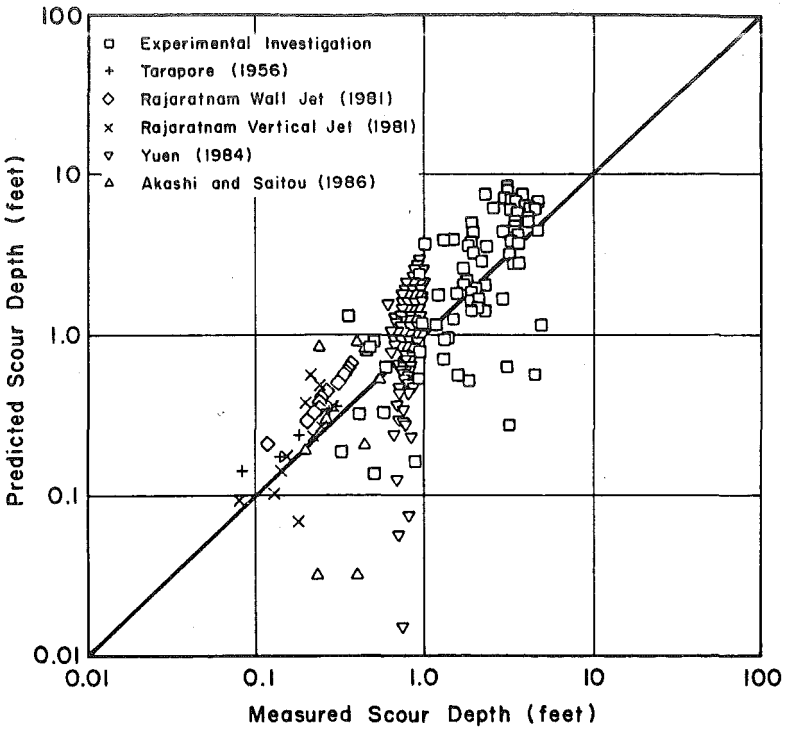

FIG. 7. Comparison of Measured and Calculated Scour Depth D_s

ically by analogy between the local scour process and jet diffusion in a plunge pool. After considering the jet trajectory, jet diffusion and stability of sediment particles in the scour hole, it is found that the exponents of the proposed equilibrium scour-depth relationship (Eq. 11) agree well with those of empirical relationships listed in Table 2. The large-scale experiments considerably extend the range of conditions for which local scour data is available. Scour depths exceeding 1.4 m (4.6 ft) were measured at unit flow discharges of 2.5 m^2/s (27 sq ft/sec). Analysis of 231 scour-depth measurements showed that the length of jet diffusion in Fig. 6 can be determined with reasonable accuracy, while Eq. 14 determines the jet angle β' with a mean prediction error of about $\pm 5°$. This explains the scatter shown in Fig. 7 for the equilibrium scour depth calculated from Eq. 11. The agreement between measured and calculated scour depths from Eq. 11 is reasonable, considering that a wide variety of conditions including vertical jets, wall jets, free overfall jets, submerged jets and flow over large-scale grade-control structures are shown in Fig. 7.

ACKNOWLEDGMENTS

The experimental investigation was completed while the first writer was employed at Simons, Li and Associates, Inc. Permission to use the data collected in this project funded by the Pima County Arizona Department of

Transportation and Flood Control District is gratefully acknowledged. The authors are thankful to E. V. Richardson and D. B. Simons for their encouragement and support during the course of this investigation.

APPENDIX I. REFERENCES

Akashi, N., and Saitou, T. (1986). "Influence of water surface on scour from vertical submerged jets." *J. Hydrosci. Hydr. Engrg.*, 55–69.

Albertson, M. L., Dai, Y. B., Jensen, R. A., and Rouse, H. (1950). "Diffusion of submerged jets." *Trans.*, ASCE, 115(2409), 639–697.

Altinbilek, H. D., and Basmaci, Y. (1973). "Localized scour at the downstream of outlet structures." *Proc., Int. Congress on Large Dams*, Madrid, Spain, 105–121.

Altinbilek, H. D., and Okyay, S. (1973). "Localized scour in a horizontal sand bed under vertical jets." *Proc., 15th Congress of Int. Association for Hydr. Res.*, Istanbul, Turkey, 99–106.

Beltaos, S., and Rajaratnam, N. (1973). "Plane turbulent impinging jets." *J. Hydr. Res.*, 11(1), 29–59.

Bogardi, J. (1974). *Sediment transport in alluvial streams*. Akademiai Kaido, Budapest, Hungary.

Bormann, N. E. (1988a). "Equilibrium local scour downstream of grade-control structures," thesis presented to Colorado State University, at Fort Collins, Colo., in partial fulfillment of the requirements for the degree of Doctor of Philosophy.

Bormann, N. E. (1988b). "Physical model of local scour at grade-control structures." *Proc., ASCE Nat. Conf. on Hydr. Engrg.*, ASCE, 1129–1134.

Bourque, C., and Newman, B. G. (1960). "Reattachment of a two-dimensional incompressible jet to an adjacent flat plate." *Aeronautical Quarterly*, 11, 201–232.

Breusers, H. N. C. (1967a). "Time scale of two-dimensional local scour." *Proc., 12th Congress of the Int. Association of Hydr. Res.*, Fort Collins, Colo., 3(32), 275–282.

Breusers, H. N. C. (1967b). "Two-dimensional local scour in loose sediment." *Closure of estuarine channels in tidal regions (Delft Hydr. Pub. No. 64)*.

Carstens, M. R. (1966). "Similarity laws for localized scour." *J. Hydr. Div.*, ASCE, 92(3), 13–34.

Chee, S. P., and Kung, T. (1971). "Stable profiles of plunge basins." *J. Am. Water Res. Assoc.*, 7(2), 303–308.

Chee, S. P., and Padiyar, P. V. (1969). "Erosion at the base of flip buckets." *Engrg. J.*, 52(111), 22–24.

Chee, S. P., Strelchuk, D. L., and Kung, T. (1972). "Configurations of water basin for energy dissipation." *86th Annual Congress of Engrg. Institute of Canada*, Saskatoon.

Chee, S. P., and Yuen, E. M. (1985). "Erosion of unconsolidated gravel beds." *Can. J. Civ. Engrg.*, 12, 559–566.

Damle, P. M., et al. (1966). "Evaluation of scour below ski jump buckets of spillways." *Golden Jubilee Symp.*, Central Water and Power Res. Station, Poona, India, 1, 154–163.

Eggenberger, W. (1943). "Die Kolkbildung bei einen Uberstromen und beider Kombination Uberstromen-Unterstromen," thesis presented to ETH, at Zurich, Switzerland, in partial fulfillment of the requirements for the degree of Doctor of Philosophy (in German).

Farhoudi, J., and Smith, K. V. H. (1985). "Local scour profiles downstream of hydraulic jumps." *J. Hydr. Res.*, 23(4), 343–358.

Hartung, W. (1959). "Die Kolkbildung hinter Überstromen wehren im Hinblick auf eine beweglich Sturzbettgestaltung." *Die Wasser Wirtschaft*, 49(1), 309–313, (in German).

Jaeger, C. (1939). "Uber die Aehnlichkeit bei flussaulichen Modellversuchen." *Wasserkraft und Wasserwirtschaft*, 34(23/24), 269, (in German).

Kobus, H., Leister, P., and Westrich, B. (1979). "Flow field and scouring effects of steady and pulsating jets impinging on a movable bed." *J. Hydr. Res.*, 17(3), 175–192.

Laursen, E. M. (1952). "Observations on the nature of scour." *Proc., 5th Hydr. Conf., Bull. 34,* Univ. of Iowa, Iowa City, Iowa, 179–197.
Laursen, E. M., and Flick, M. W. (1983). "Scour at sill structures." *Report FHWA/AZ83/184,* Arizona Transp. and Traffic Inst., Tempe, Ariz.
LeFeuvre, A. R. (1965). "Sediment transport functions with special emphasis on localized scour," thesis presented to Georgia Institute of Technology, at Atlanta, Ga., in partial fulfillment of the requirements for the degree of Doctor of Philosophy.
Martins, R. (1975). "Scouring of rocky riverbeds and free-jet spillways." *Int. Water Power Dam Constr.,* 27(5), 152–153.
Mason, P. J., and Arumugam, K. (1985). "Free jet scour below dams and flip buckets." *J. Hydr. Engrg.,* ASCE, 111(2), 220–235.
Mueller, R., and Eggenberger, W. (1944). "Experimentelle und theoretische Untersuchungen uber das Kolkproblem." *Mitt. Versuchanstalt Wasserbau,* No. 5, ETH, Zurich (in German).
Neill, C. R. (1968). "Note on initial movement of coarse uniform bed material." *J. Hydr. Res.,* 6(2), 173–176.
Newman, B. G. (1961). "The deflection of plane jets by adjacent boundaries—Coanda effect." *Boundary Layer and Flow Control,* Vol. 1, G. V. Lachman, ed., Pergamon Press, New York, N.Y.
Rajaratnam, N. (1981). "Erosion by plane turbulent jets." *J. Hydr. Res.,* 19(4), 339–358.
Rajaratnam, N., and Subramanya, K. (1968). "Plane turbulent reattached wall jets." *J. Hydr. Div.,* ASCE, 94(1), 95–112.
Schoklitsch, A. (1932). "Kolkbildung unter Uberfallstrahlen." *Wasserwirtschaft,* 343, (in German).
Smith, C. D., and Strang, D. K. (1967). "Scour in stone beds." *Proc., 12th Congress of the Int. Association for Hydr. Res.,* 65–73.
Stevens, M. A., and Simons, D. B. (1971). "Stability analysis for coarse granular material." *River Mechanics,* Vol. 1, H. W. Shen, ed., Fort Collins, Colo.
Straub, L. G. (1953). "Dredge-fill closure of Missouri River at Fort Randall." *Proc., Minnesota Hydr. Convention,* Int. Association for Hydr. Res.
Tarapore, Z. S. (1956). "Scour below a submerged sluice gate," thesis presented to the University of Minnesota, at Minneapolis, Minn., in partial fulfillment of the requirements for the degree of Master of Science.
Veronese, A. (1937). *Erosion of a bed downstream from an outlet.* Colorado A&M College, Fort Collins, Colo.
Yuen, E. M. (1984). "Clearwater scour by high velocity jets," thesis presented to the University of Windsor, at Windsor, Ontario, in partial fulfillment of the requirements for the degree of Master of Science.

APPENDIX II. NOTATION

The following symbols are used in this paper:

A', B', C', P, P' = points of interest below grade-control structures;
a, b, c, d, e, f, i = exponents of scour-depth equation;
B = coefficient of friction relationship;
C_d = jet diffusion coefficient;
C_f = local friction coefficient;
D_p = drop height of structure;
D_s = equilibrium scour depth;
d_s = sediment size;
d_{50}, d_{90} = standard sieve diameter for which 50%, 90% of particles are finer, respectively;
g = gravitational acceleration;
ΔH = head drop across structure;

K = constant in scour equation;
L_s = diffused length of jet;
q = unit water discharge;
R^2 = coefficient of determination;
U_b = diffused near bed jet velocity;
U_o = jet velocity entering tailwater;
X_s = horizontal distance to point of maximum scour;
x = exponent of friction relationship;
Y_b = jet thickness at location of maximum scour;
Y_o = jet thickness entering tailwater;
Y_t = tailwater depth;
α = maximum side angle of scour hole;
β, β' = jet angle near surface and near bed, respectively;
γ, γ_s = specific weight of water and sediment, respectively;
θ_{cr} = critical Shields number;
λ = face angle of structure;
μ, ν = dynamic and kinematic water viscosity, respectively;
ρ, ρ_s = mass density of water and sediment, respectively;
τ_b = critical shear stress at an upsloping angle α;
τ_{cr} = critical shear stress for horizontal bed; and
ϕ = submerged angle of repose of bed sediment.